European Journal of Applied Sciences – Vol. 13, No. 04
Publication Date: July 12, 2025
DOI:10.14738/aivp.1304.19070.
Sorescu, M., Corcovilos, T. A., Higinbotham, D., & Stutzman, M. (2025). Mössbauer Spectroscopy Study of $Fe_{75.3}$ $Ni_{0.8}$ $Cr_{0.9}$ $Si_{8.7}$ $B_{14.3}$ Ferromagnetic Alloy After Thermal Annealing, Laser and Electron Beam Irradiation. *European Journal of Applied Sciences*, Vol - 13(04). 13-24.

Mössbauer Spectroscopy Study of $Fe_{75.3}$ $Ni_{0.8}$ $Cr_{0.9}$ $Si_{8.7}$ $B_{14.3}$ Ferromagnetic Alloy After Thermal Annealing, Laser and Electron Beam Irradiation

Monica Sorescu
Duquesne University, Department of Physics,
Fisher Hall, Pittsburgh, PA 15282, United States

Theodore A. Corcovilos
Duquesne University, Department of Physics,
Fisher Hall, Pittsburgh, PA 15282, United States

Douglas Higinbotham
Thomas Jefferson National Accelerator Facility,
Newport News, VA 23606, United States

Marcy Stutzman
Thomas Jefferson National Accelerator Facility,
Newport News, VA 23606, United States

ABSTRACT

This paper presents a Mössbauer spectroscopy study of the behavior of $Fe_{75.3}Ni_{0.8}Cr_{0.9}Si_{8.7}B_{14.3}$ ferromagnetic alloy after thermal annealing, cw laser and high-energy electron beam irradiation. Thermal annealing at 450 ^{o}C caused structural relaxation of the alloy system, supported by an increase in the average magnetic hyperfine field and width of the field distribution, accompanied by a significant out-of-plane reorientation of the magnetic moment directions. Thermal annealing at temperatures of 550-750 ^{o}C determined crystallization of the bulk of the specimens and a-(FeNiCr), $(FeNiCr)_3$(BSi) and $(FeNiCr)_2$(BSi) crystalline phases were identified. At the highest treatment temperature, $(FeNiCr)_3$(BSi) partially decomposed into a-(FeNiCr) and $(FeNiCr)_2$(BSi). Cw laser irradiation essentially preserved the preferred in-plane orientation of the magnetic moment directions, with a slight tendency of an out-of-plane reorientation. Irradiation of the $Fe_{75.3}Ni_{0.8}Cr_{0.9}Si_{8.7}B_{14.3}$ alloy system with 11 GeV electrons maintained the in-plane direction of bulk magnetization in the beam dump sample and caused an even more pronounced in-plane direction of the magnetic moments in the target platform sample. This is due to the low value of the magnetostriction constant of the $Fe_{75.3}Ni_{0.8}Cr_{0.9}Si_{8.7}B_{14.3}$ system. Both laser and electron beam irradiation were demonstrated to keep the amorphous phase of the $Fe_{75.3}Ni_{0.8}Cr_{0.9}Si_{8.7}B_{14.3}$ alloy, making it a strong candidate for radiation-resistant materials.

Keywords: amorphous ferromagnetic alloys, thermal annealing, laser irradiation, electron beam irradiation, Mössbauer spectroscopy.

INTRODUCTION

Amorphous ferromagnetic alloys (often called metallic glasses) are fascinating materials that combine the magnetic properties of ferromagnets with the structural disorder of glasses [1-8]. Unlike metals, these alloys have a disordered atomic structure, which eliminates grain boundaries and defects. They exhibit low coercivity, high magnetic permeability, and low core losses, making them excellent soft magnetic materials. Their high electrical resistivity reduces eddy current losses, especially at high frequencies. The alloys' structure gives them superior mechanical strength and resistance to deformation and many compositions show excellent resistance to oxidation and corrosion.

A significant number of studies [9-20] have identified Mössbauer spectroscopy as the technique of choice for the characterization and description of the phase composition and magnetic properties of the ferromagnetic alloys after different types of processing. Recently, FeNiCrBSi compositions have been investigated in the amorphous state only [21] and nothing is known about the behavior of the alloy under thermal annealing or irradiation with laser and particle beams. The latter provide unconventional pathways for the amorphous-to-crystalline phase transformation of the metallic glass and test the suitability of the system for the development of radiation-resistant materials.

In this study we present a comprehensive Mössbauer spectroscopy characterization of an $Fe_{75.3}Ni_{0.8}Cr_{0.9}Si_{8.7}B_{14.3}$ amorphous ferromagnetic alloy in the as-quenched state and after thermal annealing in the range 450-750^{o}C, cw CO_2 laser and 11 GeV electron beam irradiation. Critical information on the phase composition and magnetic texture was obtained from the transmission Mössbauer spectra and the magnetic hyperfine field distributions extracted from them.

MATERIALS AND METHODS

Amorphous ferromagnetic alloy with the composition $Fe_{75.3}Ni_{0.8}Cr_{0.9}Si_{8.7}B_{14.3}$ was obtained by rapid quenching from the melt by Spang Co. using a conventional melt-spinning technique. The as-obtained alloy had the following parameters: maximum induction B_{max}=1.5 T, magnetostriction constant l_s=12 ppm, magnetic permeability m=7000, Curie temperature T_c=460^{o} C and density g=7.38 g/cm^3. Samples cut from the ribbon foils were isochronally processed at 450, 550, 650 and 750^{o} C in a thermal annealing furnace for 1 hour.

As-quenched amorphous samples were subjected to a model Synrad 48-2 cw CO_2 laser having the wavelength of 10 mm, delivering a power of 25 W with a beam radius of 0.14 mm. Irradiation was performed for a time of 30 ms/spot with small overlaps, providing a laser energy density of about 10 J/mm^2 on the samples. In a different experiment, the foils were exposed to the prompt high radiation environment created by an 11 GeV electron beam incident on the foils in Hall C at the Thomas Jefferson National Accelerator Facility. A uniform dose of 0.1 Mrad of ionizing radiation was received by both beam dump and target platform foils. The radiation dose was determined using special dosimeters located with the samples.

A SeeCo model W302 constant acceleration spectrometer using a ^{57}Co gamma ray source diffused in a Rh matrix was used to perform room temperature transmission Mössbauer measurements. The spectra were analyzed with the WINormos SITE and DIST package of

programs, which provided the hyperfine magnetic field parameters as well as the distributions extracted from the spectra after least-squares fitting.

RESULTS AND DISCUSSION

Figure 1 (a) shows the room temperature transmission Mössbauer spectrum of the $Fe_{75.3}Ni_{0.8}Cr_{0.9}Si_{8.7}B_{14.3}$ amorphous ferromagnetic alloy in the as-quenched state. The six-line pattern is due to the nuclear Zeeman effect and exhibits broadened resonances, due to fluctuations of the hyperfine parameters from site-to-site in the amorphous structure. These fluctuations give rise to a magnetic hyperfine field distribution, which is described by the plot given in Figure 1 (b).

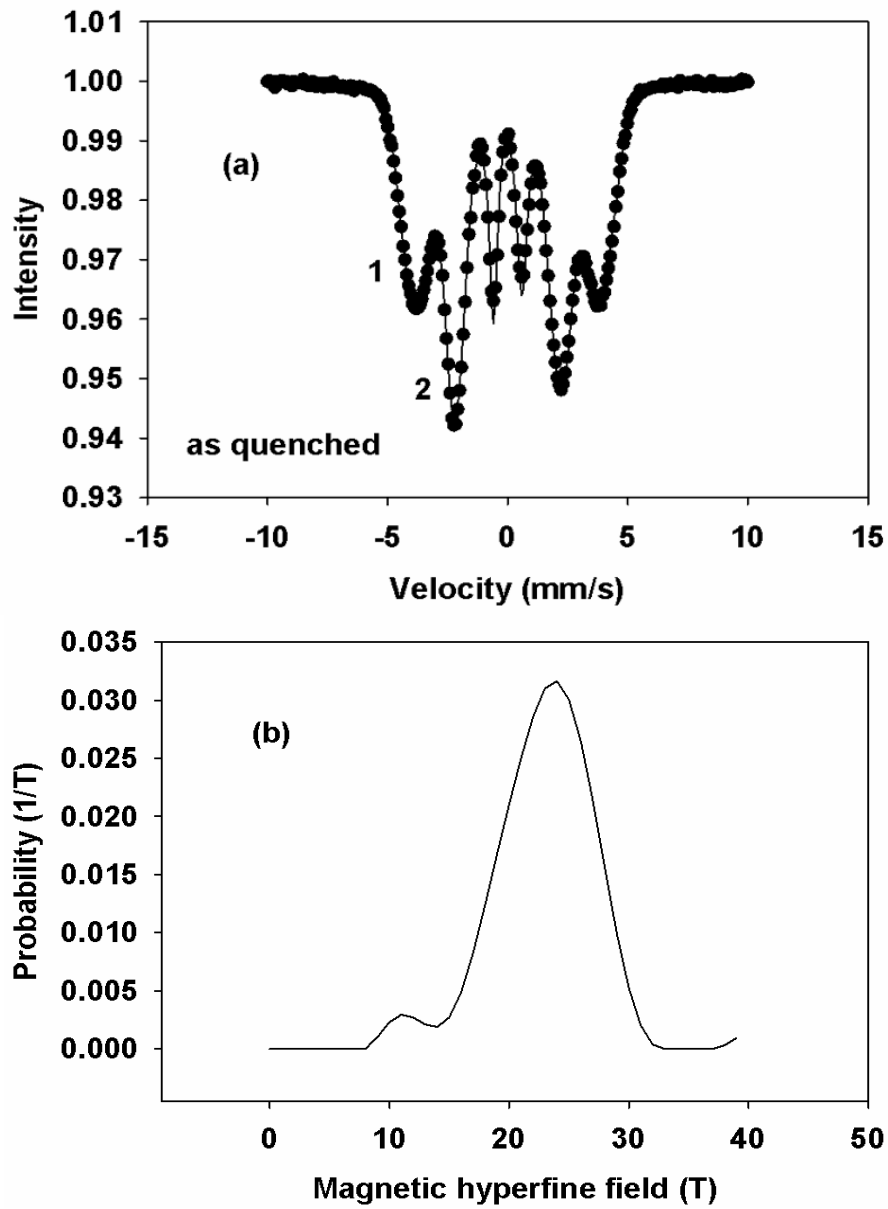

Fig 1: Transmission Mössbauer spectrum of the $Fe_{75.3}Ni_{0.8}Cr_{0.9}Si_{8.7}B_{14.3}$ ferromagnetic alloy (a) in the amorphous as-quenched state and (b) the corresponding magnetic hyperfine field distribution.

The relative intensity of lines 2 to 1 in the amorphous spectrum is given by $R_{21}=4\sin^2 a/[3(1+\cos^2 a)]$, where a is the angle between the magnetic moment direction and the direction of propagation of the gamma rays. R_{21} takes values from 0 to 4/3 when a changes from 0 to 90° and for a completely random distribution of the magnetic moment directions takes the value 0.67. We can introduce the angle q=90°-a as the angle between the average direction of the magnetic moments and the sample plane. The least-squares fitted values of the magnetic texture parameter R_{21} and angle q of 25.59° are listed in Table 1 and are consistent with a preferred in-plane orientation of the magnetic moment direction in the as-quenched specimen, close to the sample surface. The average magnetic hyperfine field $<B_{hf}>$ of 22.82 T and width of the field distribution DB_{hf}=5.27 T were extracted from the spectrum at the same time with the least-squares fitting and are in a range typical for ferromagnetic alloys. The magnetic hyperfine field distribution is bimodal, in excellent agreement with that given in [21] for a series of FeNiCrSiB amorphous alloy compositions.

Figure 2 (a) shows the room temperature transmission Mössbauer spectrum of the $Fe_{75.3}Ni_{0.8}Cr_{0.9}Si_{8.7}B_{14.3}$ ferromagnetic alloy after thermal annealing at 450° C for 1 hour and Figure 2 (b) displays the magnetic hyperfine field distribution extracted from this spectrum. The angle q of 33.56° indicates a pronounced out-of-plane reorientation of the magnetic moment direction. Moreover, the increase in the average magnetic hyperfine field to $<B_{hf}>$ of 23.52 T and width of the field distribution to DB_{hf} of 5.57 T (Table 1) are consistent with the process of structural relaxation of the as-quenched amorphous as effect of the thermal annealing performed.

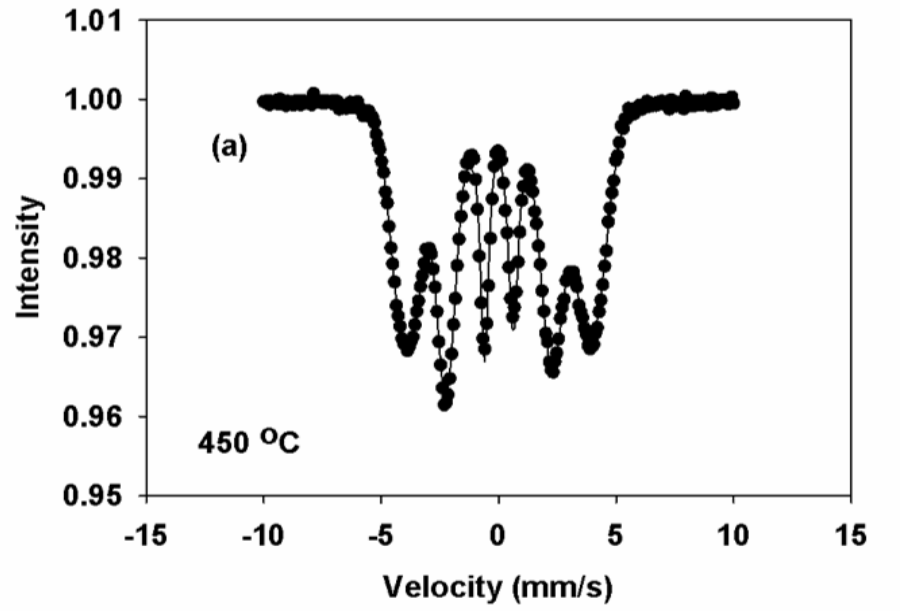

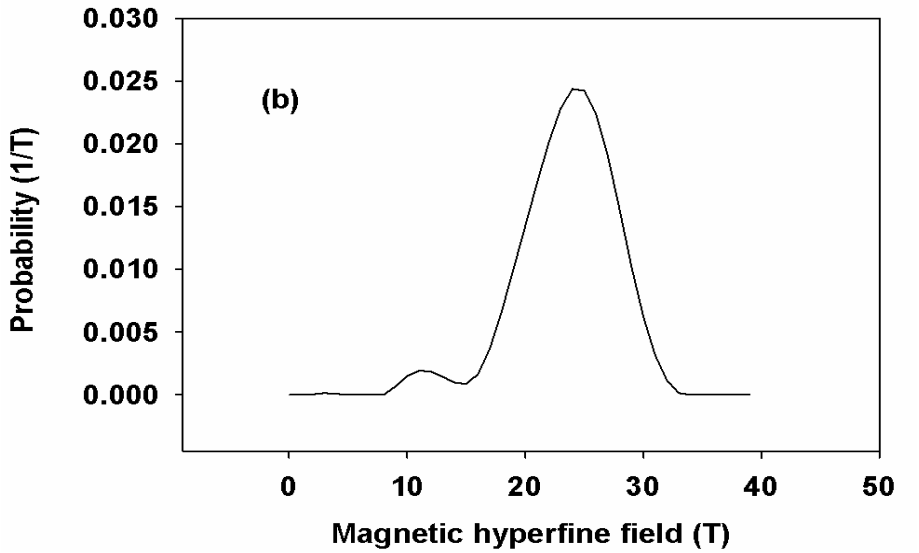

Fig 2: Transmission Mössbauer spectrum of the $Fe_{75.3}Ni_{0.8}Cr_{0.9}Si_{8.7}B_{14.3}$ ferromagnetic alloy (a) annealed at a temperature of 450° C and (b) the corresponding magnetic hyperfine field distribution.

Table 1: Mössbauer parameters of $Fe_{75.3}Ni_{0.8}Cr_{0.9}Si_{8.7}B_{14.3}$ amorphous ferromagnetic alloy (relative intensity of lines, average magnetic moment direction, average magnetic hyperfine field and width of the field distribution)

Sample	R_{21}	θ (deg)	$<B_{hf}>$ (T)	ΔB_{hf} (T)
as quenched	0.914	25.59	22.82	5.27
450 °C	0.709	33.56	23.52	5.57
cw laser	0.903	26.01	23.04	5.38
beam dump	0.920	25.35	22.92	5.36
target platform	0.960	23.79	22.94	5.36
Errors	±0.001	±0.01	±0.01	±0.01

Figures 3, 4 and 5 present the room-temperature transmission Mössbauer spectra for the $Fe_{75.3}Ni_{0.8}Cr_{0.9}Si_{8.7}B_{14.3}$ ferromagnetic alloy after thermal annealing for 1 hour at 550, 650 and 750° C, respectively. The refined values of the hyperfine parameters extracted from these spectra are given in Table 2.

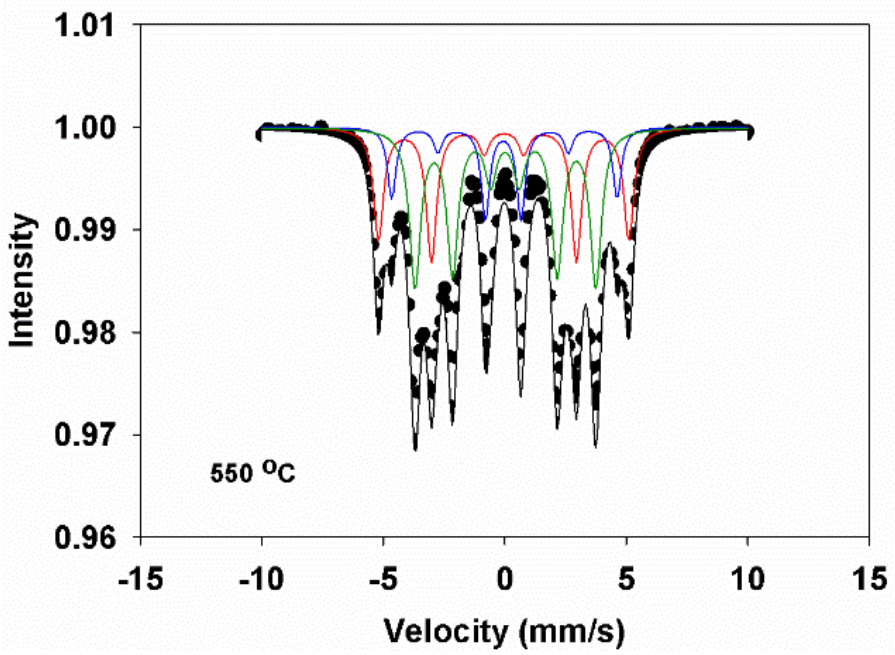

Fig 3: Transmission Mössbauer spectrum of the Fe75.3Ni0.8Cr0.9Si8.7B14.3 ferromagnetic alloy annealed at a temperature of 550o C.

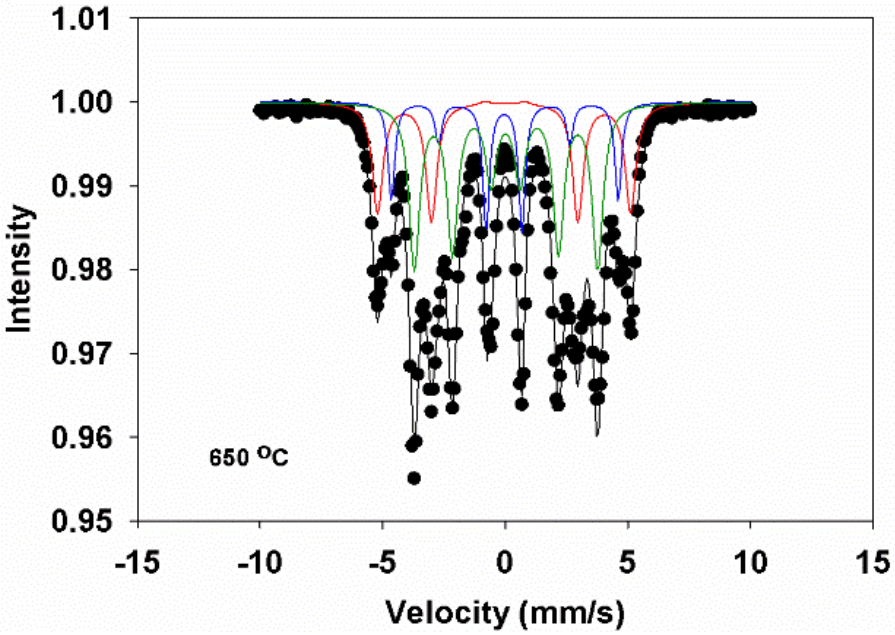

Fig 4: Transmission Mössbauer spectrum of the Fe75.3Ni0.8Cr0.9Si8.7B14.3 ferromagnetic alloy annealed at a temperature of 650o C.

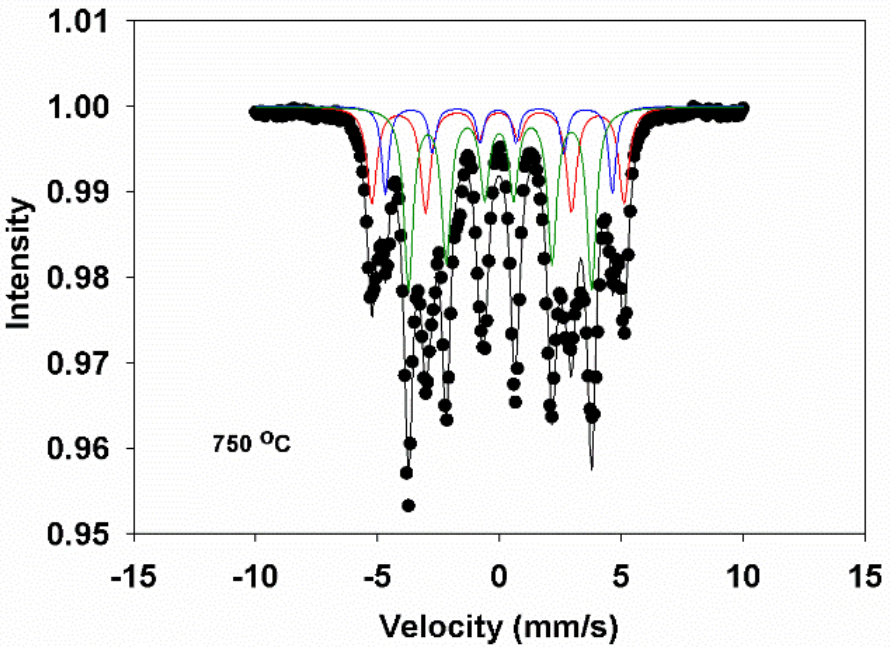

Fig 5: Transmission Mössbauer spectrum of the Fe75.3Ni0.8Cr0.9Si8.7B14.3 ferromagnetic alloy annealed at a temperature of 750o C.

Table 2: Mössbauer parameters of $Fe_{75.3}Ni_{0.8}Cr_{0.9}Si_{8.7}B_{14.3}$ annealed ferromagnetic alloy (magnetic hyperfine field, isomer shift vs. Fe, quadrupole shift, relative areas, assignment of phases)

Sample	B_{hf} (T)	δ (mm/s)	2ε (mm/s)	Relative areas (%)	Assignment of phases
550 °C	31.95	0.076	-0.012	32.8	α-(FeNiCr)
	28.75	0.076	0.053	15.4	$(FeNiCr)_3(BSi)$
	23.08	0.097	0.021	51.8	$(FeNiCr)_2$ (BSi)
650 °C	31.98	0.078	-0.026	31.1	α-(FeNiCr)
	28.67	0.080	0.030	15.1	$(FeNiCr)_3(BSi)$
	23.16	0.132	0.020	53.8	$(FeNiCr)_2(BSi)$
750 °C	32.07	0.073	-0.026	33.9	α-(FeNiCr)
	28.89	0.080	0.030	11.3	$(FeNiCr)_3(BSi)$
	23.28	0.129	0.038	54.8	$(FeNiCr)_2(BSi)$
Errors	±0.01	±0.001	±0.001	±0.1	

The sharp resonances in the spectra are consistent with the onset of bulk crystallization in the thermally annealed alloy samples. All spectra were fitted with three sextets, corresponding to a-(FeNiCr), $(FeNiCr)_3(BSi)$ and $(FeNiCr)_2(BSi)$ crystalline phases. Phase identification was

performed based on the values of the magnetic hyperfine fields and isomer shifts. At the highest annealing temperature, $(FeNiCr)_3(BSi)$ partially decomposed into a-(FeNiCr) and $(FeNiCr)_2(BSi)$, as shown by the trend in the relative areas.

Figure 6 (a) shows the room temperature Mössbauer spectrum of the $Fe_{75.3}Ni_{0.8}Cr_{0.9}Si_{8.7}B_{14.3}$ ferromagnetic alloy after irradiation with the cw CO_2 laser and Figure 6 (b) presents the magnetic hyperfine field distribution extracted from the spectrum.

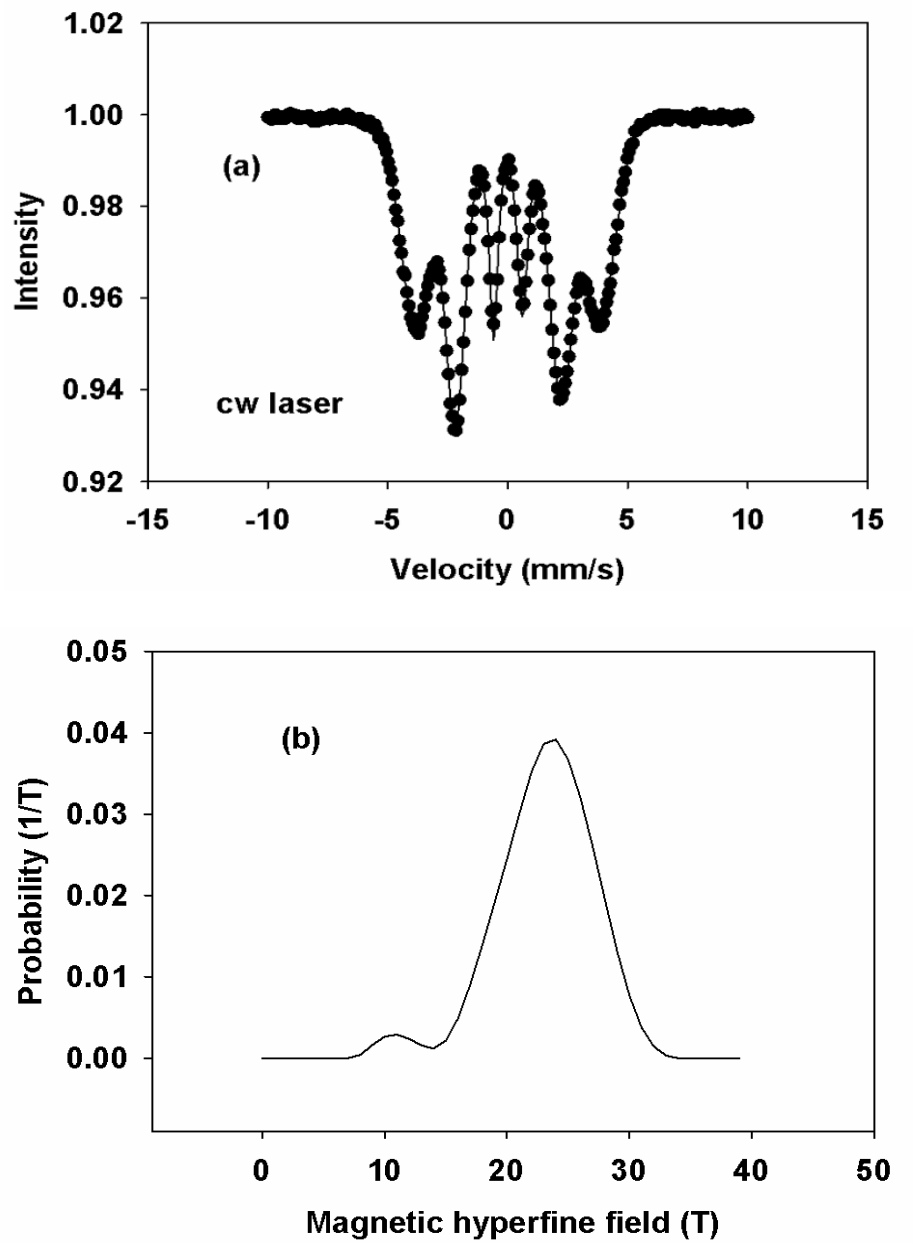

Fig 6: Transmission Mössbauer spectrum of the $Fe_{75.3}Ni_{0.8}Cr_{0.9}Si_{8.7}B_{14.3}$ ferromagnetic alloy (a) after cw laser irradiation and (b) the corresponding magnetic hyperfine field distribution.

As can be seen in Table 1, the average magnetic hyperfine field increases to 23.04 T and the width of the field distribution also increases to 5.38 T, results which are consistent with a

degree of structural relaxation of the as-quenched amorphous, known to precede the onset of crystallization in the irradiated specimen. The average angle q describing the direction of bulk magnetization increases to 26.01°, which shows that the magnetic moment directions maintain a preferred in-plane orientation, with a slight tendency of rotation out of the ribbon plane. These results show that cw laser processing essentially preserves the amorphous nature of the $Fe_{75.3}Ni_{0.8}Cr_{0.9}Si_{8.7}B_{14.3}$ ferromagnetic alloy system.

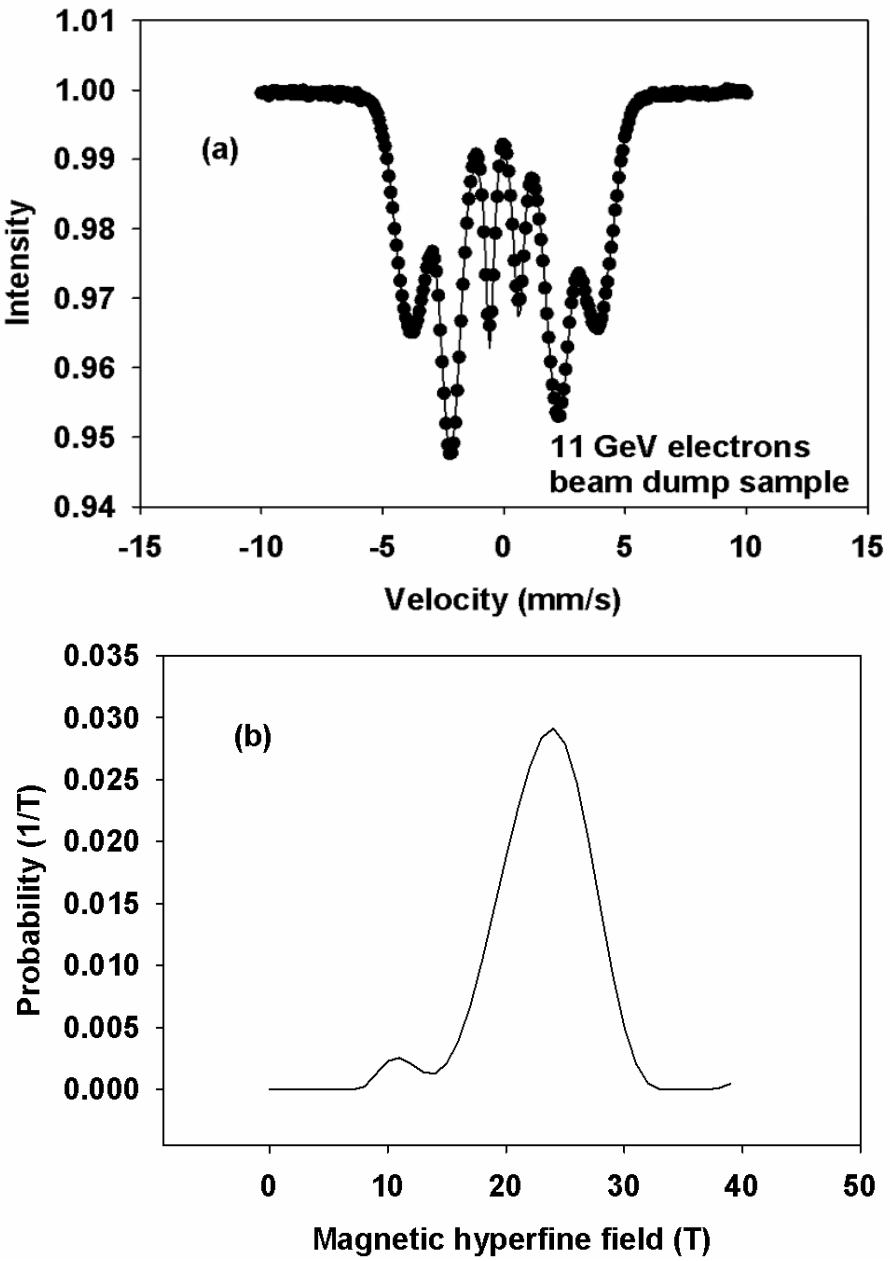

Fig 7: Transmission Mössbauer spectrum of the $Fe_{75.3}Ni_{0.8}Cr_{0.9}Si_{8.7}B_{14.3}$ ferromagnetic alloy (a) beam dump sample after 11 GeV electron beam irradiation and (b) the corresponding magnetic hyperfine field distribution.

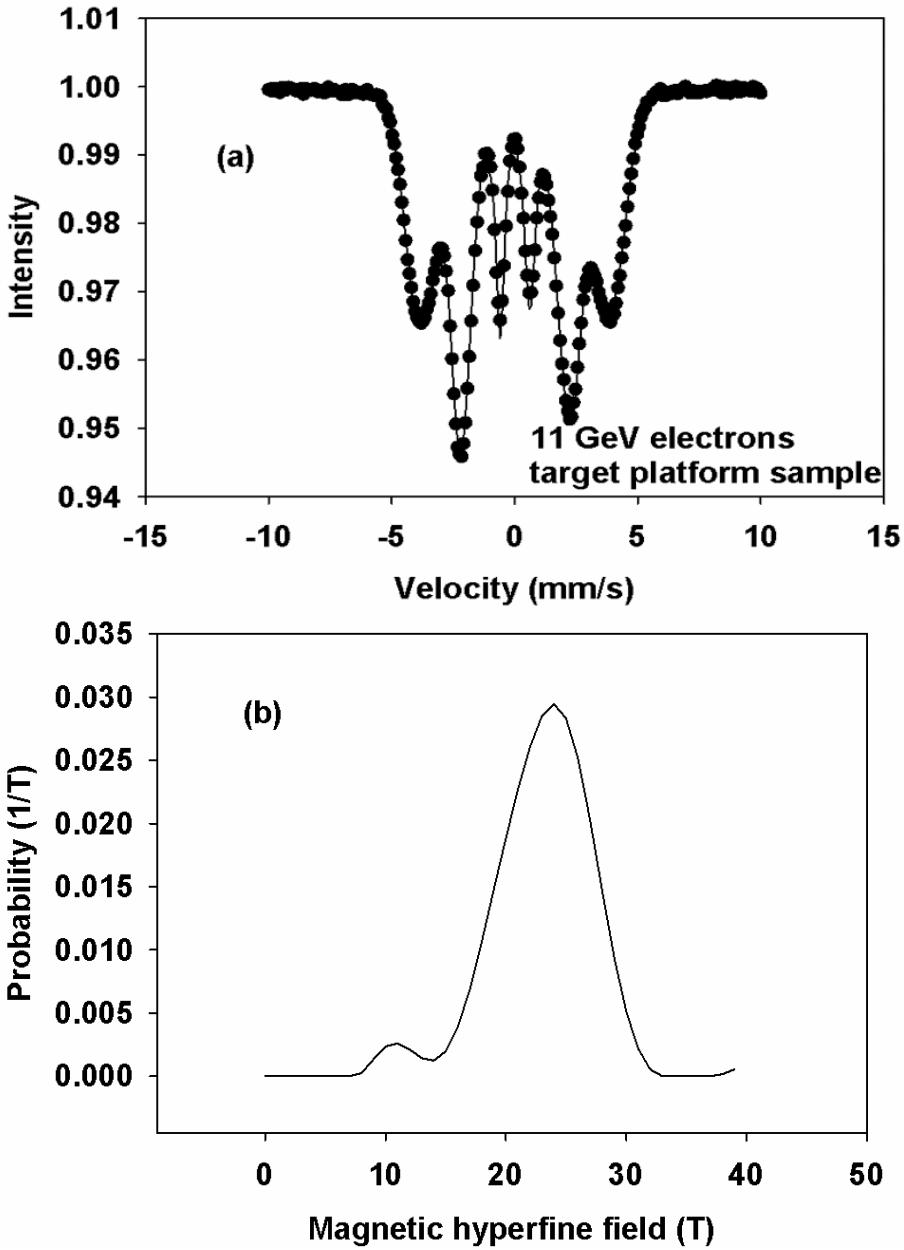

Fig 8: Transmission Mössbauer spectrum of the $Fe_{75.3}Ni_{0.8}Cr_{0.9}Si_{8.7}B_{14.3}$ ferromagnetic alloy (a) target platform sample after 11 GeV electron beam irradiation and (b) the corresponding magnetic hyperfine field distribution.

Figure 7 (a) shows the room temperature transmission Mössbauer spectrum of the $Fe_{75.3}Ni_{0.8}Cr_{0.9}Si_{8.7}B_{14.3}$ beam dump ferromagnetic alloy sample after irradiation with 11 GeV electrons and Figure 7 (b) displays the magnetic hyperfine field distribution obtained from the spectrum. Both the average magnetic hyperfine field and width of the field distribution show small increases to 22.92 and 5.36 T, respectively, but the angle q maintains the in-plane orientation of the as-quenched amorphous (Table 1). Figure 8 (a) presents the room temperature transmission Mössbauer spectrum of the $Fe_{75.3}Ni_{0.8}Cr_{0.9}Si_{8.7}B_{14.3}$ target platform alloy sample after irradiation with 11 GeV electrons and Figure 8 (b) presents the magnetic hyperfine field distribution extracted from the spectrum. While the average magnetic

hyperfine field and width of the field distribution (Table 1) exhibit small increases to 22.94 and 5.36 T, respectively, the value of the angle q of 23.79^o suggests an even more pronounced in-plane direction of the magnetic moments compared to the as-quenched specimen. This result can be ascribed to the low value of the magnetostriction constant of the $Fe_{75.3}Ni_{0.8}Cr_{0.9}Si_{8.7}B_{14.3}$ alloy of only 12 ppm, such that the magnetoelastic effects cannot cause an out-of-plane reorientation of the magnetic moment directions as in the case of the highly magneto strictive $Fe_{56}Co_{24}Nb_4B_{13}Si_2Cu_1$ composition studied previously [22]. Just as in the case of laser irradiation, these results show that high-energy electron beam irradiation essentially preserves the amorphous phase of the alloy and recommends it for radiation-resistant materials applications. While other techniques such as electron microscopy and X-ray diffraction cannot provide useful information, it may be noted that Mössbauer spectroscopy is a powerful tool, able to detail subtle changes in the structural and magnetic parameters of the irradiated alloys.

CONCLUSIONS

This paper provides a comprehensive Mössbauer spectroscopy investigation of the $Fe_{75.3}Ni_{0.8}Cr_{0.9}Si_{8.7}B_{14.3}$ amorphous ferromagnetic alloy subjected to thermal annealing, laser and high-energy electron beam irradiation. Thermal annealing at a temperature of 450^o C was found to induce structural relaxation in the alloy sample. Thermal treatment at temperatures in the range 550-750^o C caused amorphous-to-crystalline phase transformation in the alloy and a-(FeNiCr), $(FeNiCr)_3(BSi)$ and $(FeNiCr)_2(BSi)$ crystalline phases were identified. Cw laser irradiation was found to preserve the in-plane orientation of the magnetic moments, with a slight tendency for an out-of-plane direction. Irradiation with 11 GeV electrons induced an even more pronounced in-plane orientation of the average direction of bulk magnetization. Unlike thermal treatment, irradiation by laser and electron beams is more likely to preserve the amorphous phase of the alloy, making it an intriguing candidate for radiation-resistant materials.

ACKNOWLEDGMENTS

This work was supported by the National Science Foundation, US under grants number DMR-0854794 and DMR-1002627-1. We thank Michael Van Stipdonk for access to the CO_2 laser.

Conflict of interests

The authors acknowledge that there are no conflicts of interest regarding this paper.

References

1. Torrens-Serra, J., et al., Effect of minor additions on the glass forming ability and magnetic properties of Fe-Nb-B based metallic glasses. Intermetallics, 2010. 18: p. 773-780.
2. Chen, N., et al., A new class of non-crystalline materials: Nanogranular metallic glasses. Journal of Alloys and Compounds, 2017. 707: p. 371-378.
3. Ziewiec, K., et al., Formation and microstructure of the amorphous/crystalline $Fe_{55}Ni_{20}Cu_5P_{10}Si_5B_5$ composite produced by two-component melt-spinning. Journal of Alloys and Compounds, 2018. 750: p. 471-478.
4. Gutierrez, J., et al., Induced anisotropy and magnetoelastic properties in Fe-rich metallic glasses. Journal of Non-Crystalline Solids, 2001. 287: p. 417-420.
5. Torrens-Serra, J., et al., Influence of composition in the crystallization process of $Fe_{75-x}Nb_{10}B_{15+x}$ metallic glasses. Journal of Non-Crystalline Solids, 2007. 353: p. 842-844.

6. Torrens-Serra, J., et al., Glass forming ability, thermal stability, crystallization and magnetic properties of $[(Fe, Co, Ni)_{0.75}Si_{0.05}B_{0.20}]_{95}Nb_4Zr_1$ metallic glasses. Journal of Non-Crystalline Solids, 2013. 367: p. 30-36.
7. Dai, J., et al., Structural aspects of magnetic softening in Fe-based metallic glass during annealing. Scripta Materialia, 2017. 127: p. 88-91.
8. Liu, D.Y., et al., Preparation, thermal stability, and magnetic properties of Fe-Co-Zr-Mo-W-B bulk metallic glass. Journal of Alloys and Compounds, 2004. 370: p. 249-253.
9. Torrens-Serra, J., et al., Glass-forming ability and microstructural evolution of $[(Fe_{0.6}Co_{0.4})_{0.75}Si_{0.05}B_{0.20}]_{96-x}Nb_4M_x$ metallic glass studied by Mössbauer spectroscopy. Journal of Alloys and Compounds, 2017. 704: p. 748-759.
10. Kane, S.N., et al., Mössbauer and magnetic studies of $(Fe_{100-x}Co_x)_{62}Nb_8B_{30}$ (x=0, 33, 50) alloys. Journal of Magnetism and Magnetic Materials, 2005. 292: p. 447-452.
11. Kane, S.N., et al., Influence of Nb addition on the structural and magnetic properties of FeNbAlGaPCB metallic glasses. Journal of Magnetism and Magnetic Materials, 2005. 290-291: p. 1461-1464.
12. Bhagat, N., et al., Effect of annealing on the structural and magnetic properties of $(Fe_{1-x}Co_x)_{83}B_{17}$ metallic glasses. Journal of Magnetism and Magnetic Materials, 2015. 381: p. 332-336.
13. Lashgari, H.R.. et al., Stress-relaxation heat treatment in FeSiBNb amorphous alloy: Thermal, microstructure, nanomechanical and magnetic texture measurements. Journal of Magnetism and Magnetic Materials, 2018. 456: p. 62-70.
14. Liang, X.B., et al., Mössbauer study on amorphous and nanocrystalline $(Fe_{1-x}Co_x)_{86}Hf_7B_6Cu_1$ alloys. Materials Characterization, 2007. 58: p. 143-147.
15. Tiwari, G.P., et al., Structural relaxation in metallic glasses. Materials Science and Engineering A, 2001. 304-306: p. 499-504.
16. Ile, D.C., et al., Thermal stability and crystallization behavior of $Fe_{77}C_5B_4(AlGa)_3(PSi)_{11}$ metallic glasses. Materials Science and Engineering A, 2004. 375-377: p. 297-301.
17. Bandyopadhyay, D. Mössbauer spectroscopic study of the effect of annealing on the hyperfine field distributions in $Fe_{78}B_{13}Si_9$ metallic glass. Solid State Communications, 1999. 109: p. 611-614.
18. Lu, Y., et al., Mössbauer study of the ultrahigh glass-forming ability in FeCoCrMoCBY alloy system. Vacuum, 2017. 141: p. 173-175.
19. Sorescu, M., et al., 2 GeV electron beam irradiation effects in advanced metallic glasses. Journal of Minerals and Materials Characterization and Engineering, 2022. 10: p. 106-112.
20. Sorescu, M. Recent applications of the Mössbauer effect; Dorrance Publishing Company: Pittsburgh, USA, 2020.
21. El Boubekri, A., et al., Mössbauer analysis of (FeNiCrSiB) amorphous alloy ribbons. Physica B: Condensed Matter, 2024. 691: 416374.
22. Sorescu, M., et al, Stimulating the amorphous structure of $Fe_{56}Co_{24}Nb_4B_{13}Si_2Cu_1$ ferromagnetic alloy by thermal annealing, laser and electron beam irradiation: A Mössbauer spectroscopy investigation. Journal of Alloys and Metallurgical Systems, 2023. 4: 100045.